



ELSEVIER

Journal of Luminescence 98 (2002) 15–22

JOURNAL OF
LUMINESCENCE

www.elsevier.com/locate/jlumin

Photoluminescence from single silicon quantum dots at room temperature

Jan Valenta^{a,c,*}, Robert Juhasz^b, Jan Linnros^b

^a Department of Chemical Physics and Optics, Faculty of Mathematics and Physics, Charles University, Ke Karlovu 3 CZ-121 16 Prague 2, Czech Republic

^b Department of Microelectronics and Information Technology, Royal Institute of Technology, Electrum 229, S-164 21 Kista-Stockholm, Sweden

^c Photosynthesis Research Center, University of South Bohemia, Branišovská 31, CZ-370 05 České Budějovice, Czech Republic

Abstract

Photoluminescence (PL) from single silicon quantum dots-nanocrystals (NCs) has been detected and spectrally resolved at room temperature. The Si-NCs, fabricated using electron-beam lithography, reactive ion etching, and two-step oxidation are organized in a regular matrix which enable for repeated observation of a specific single NC. The PL spectrum of a single-NC is formed by a broad band (FWHM of 120 meV or more), in which a quasi-periodic modulation (period of ~ 80 meV) appears for some NCs. The emission is polarized in arbitrary directions suggestive of geometrical differences in shape of NCs. The quantum efficiency of PL has been estimated from both saturated and non-saturated PL signal to reach as much as 35%. However only a few percent from total number of NCs shows detectable PL. Our experiments demonstrate the feasibility of PL spectroscopy of single semiconductor NCs in materials with very low emission rate (indirect band gap semiconductors). © 2002 Elsevier Science B.V. All rights reserved.

PACS: 78.67.Hc; 81.16.Nd; 78.55.Ap; 81.07.Ta

Keywords: Nanocrystals; Photoluminescence; Silicon; Lithography; Imaging spectroscopy

1. Introduction

Semiconductor nanocrystals (NC), the so-called quantum dots (QD) are potential building blocks of future nanoelectronics and nanophotonics. The current microelectronic technology should reach feature sizes on chip of about 20–30 nm by the year 2016. Below this limit the transport, electronic, and optical properties of bulk silicon start to be

influenced significantly by quantum confinement effects. Therefore, it is desirable to develop techniques of fabrication of silicon NCs (Si-NCs) and study their physical properties.

The second reason for intensive investigation of Si nanostructures is their potential application in light-emitting devices integrated on a chip. Compared to the weak IR luminescence of bulk silicon (observed only at low temperatures), the efficiency of Photoluminescence (PL) from Si nanostructures is increased enormously. The PL mechanism has been intensively debated and many different models proposed: recombination of

*Corresponding author: Tel.: +420-2-21-91-12-72, fax: +420-2-21-91-12-49.

E-mail address: jan.valenta@mff.cuni.cz (J. Valenta).

quantum confined electron–hole pairs, recombination in siloxenes, amorphous phase of Si, surface states related to silicon–oxygen or hydrogen bonds [1], etc. However, detailed studies of the PL mechanism are hampered by the broad PL band resulting from inhomogeneous broadening (omnipresent in ensembles of NCs). Although certain improvement can be achieved by size-selection methods [2] single-dot spectroscopy (SDS) would be needed to reveal the PL mechanism.

The technique of SDS measurements of individual NCs which is nowadays widely applied to study NCs of III–V and II–VI semiconductors [3] has revealed several intriguing phenomena such as PL intermittence, spectral diffusion and Stark effects [4,5]. Many of these phenomena seem to be explained by charging of the QD at high excitation power resulting in a local electric field [6]. (Accurate control of charging effects is, indeed, a key issue for the development of nanoelectronics.)

The application of the SDS to study light emission from Si-NCs is complicated by two main reasons:

- Very low emission rate: It is a consequence of the indirect band gap structure, which is conserved, even in very small Si-NCs [7]. Therefore, momentum-conserving phonons have to participate in optical transition and the radiative lifetime is very long (typically about 0.1 ms at room temperature (RT) [8]).
- Difficult fabrication of structures in which Si-NCs are well defined, efficiently emitting and have small enough concentration in order to enable detection of PL from one NC.

Up to now the only published application of SDS to Si nanostructures concerns single porous-Si grains (dispersed in liquid and deposited on the glass substrate [9]). In these samples an exceptionally high quantum efficiency of $> 50\%$ was found [10] and recently existence of one or more (up to 4) luminescing chromophores (small NCs) in a single porous-Si grain was demonstrated [11].

In our paper we present single-dot PL spectra of individual Si-NCs measured at RT. We have taken an entirely different approach in isolating the NCs

using electron-beam lithography and plasma etching to produce a regular matrix of Si pillars, followed by size reduction in the two-stage oxidation. Consequently, we are able to identify luminescing pillars and verify that the PL indeed originates from these structures. We also demonstrate PL intermittence, verifying the single PL center character, and polarization effects suggesting geometrical variations of NC shape.

2. Sample preparation and experimental set-up

Electron beam lithography was used to form resist dots with diameters as small as 50 nm on an N-type ($\langle 100 \rangle$, 20–40 Ω cm) Si wafer having a 25 nm thermal oxide layer. Reactive ion etching (RIE) using CHF_3/O_2 -based chemistry was then performed to etch through the top SiO_2 layer followed by chlorine based RIE for Si etching. The resulting 200 nm tall pillars were subsequently thermally oxidized for 5 h in O_2 gas at 850°C or 900°C. The different temperatures give slightly different consumption of Si, which combined with the range of different initial pillar diameters resulted in Si cores of different sizes ranging down to the few-nanometer regime. The oxide was then removed by buffered wet etching and the samples imaged by SEM (see Fig. 1). A second oxidation followed at 1000°C for 12 min. Finally, the samples were annealed for 30 min at 400°C in a 1:9 mixture of $\text{H}_2:\text{N}_2$ gas to passivate surface states in order to enhance the PL.

The crucial point for achieving detectable PL is to find optimal combination of the initial size of crystals (in our case it was 100 or 130 nm) and the oxidation parameters. Both wider and narrower pillars have no detectable PL as their Si core is either too big or it is completely consumed. Note that a phenomenon of self-limiting oxidation [12] plays probably very important role in the formation of a Si-NC from a pillar. The rate of oxidation is significantly reduced on a few nanometer scale when the surface has a large curvature and stress builds up at the oxide–silicon interface. For pillar geometry, the largest curvature is at the top and one may therefore expect that an isolated

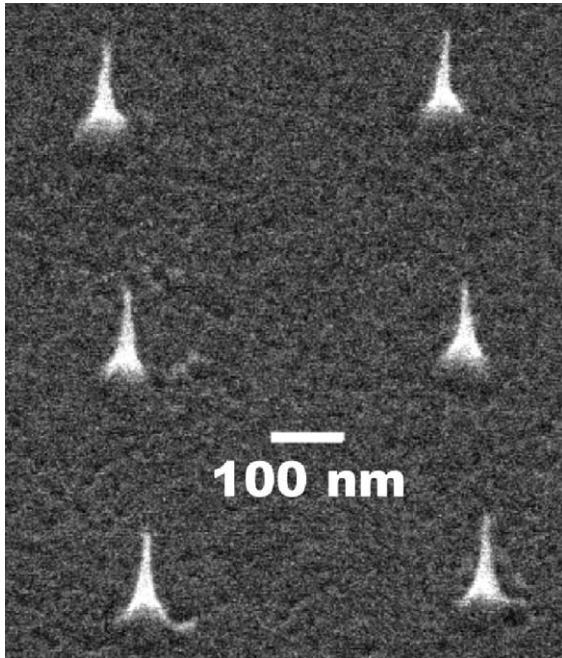


Fig. 1. SEM images (45° tilt view) of Si nanopillars after initial patterning and size-reduction by the first oxidation step.

SiO₂-embedded Si-NC could remain here while other parts of the silicon core have been oxidized.

PL images and spectra of Si-NCs were studied using an imaging spectrometer connected to a conventional optical (far-field) microscope. The light emitted from a sample was collected by an objective, imaged on the entrance slit of the spectrometer and detected at the output by a liquid nitrogen-cooled CCD camera. Reflection images of studied structures were detected under illumination with the blue (442 nm) line of a cw He–Cd laser while PL was excited by the UV line (325 nm) of the same laser. The laser beam was directed towards the sample through the gap between the objective and the sample surface at grazing incidence.

3. Experimental results and discussion

The sequence of measurements is illustrated in Fig. 2. First, the images of reflection (Fig. 2A) and PL (Fig. 2B) are detected using a mirror inside the

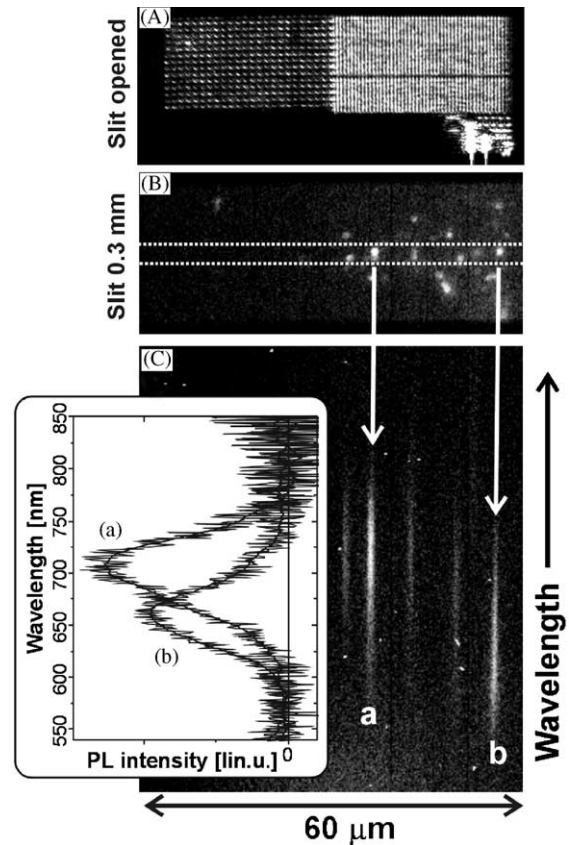


Fig. 2. The principle of imaging spectroscopy of single Si-NCs: Reflection (A) and PL (B) images of the same part of regular lattice of Si-NCs. Distance between neighbor NCs is 1 and 0.5 μm for the left and right side of the sample, respectively. The dashed white rectangle indicates the size of the entrance slit during the measurement of PL spectra. When the mirror inside spectrometer is replaced by a diffraction grating, PL spectra of single shining dots are detected as light traces on the CCD (panel C). The inset shows extracted PL spectra of the two most intensively emitting NCs (traces a and b).

spectrometer (entrance slit opened to maximum). Then, an area of interest with brightly emitting NCs has to be placed in the center of image, the entrance slit closed to desired width (resolution) and the mirror substituted by a diffraction grating in order to record a spectrum. The PL spectra are extracted from intensity profiles of light traces on the CCD (Fig. 2C) and corrected for the spectral sensitivity of the detection system.

The spatial resolution d of our imaging system is limited by diffraction $d = 1.22\lambda(2NA)^{-1}$, where λ

is the used wavelength and NA the numerical aperture. In our case ($NA = 0.7$), the resolution is about 500 nm in reflection and slightly worse in PL (see Fig. 2A and B). However, we can often resolve the PL from individual NCs even in the case where NC spacing is on the limit of resolution ($0.5 \mu\text{m}$ right-hand side of the Fig. 2A and B) because only a small fraction of dots is shining.

PL spectra of individual Si-NCs can be measured at RT for the most intensively luminescing NCs. In Fig. 3, we plot PL spectra of three different dots. The detection time was 30 min at the excitation intensity of 0.5 W/cm^2 (the spectral resolution is about 10 nm). The PL spectrum of a single Si-NC is formed by a single band, which can be fitted by a single Gaussian peak lying in the range 1.58–1.88 eV (660–785 nm). Results of fits are plotted by bold black lines in Fig. 3. Full-width at half-maximum (FWHM) is 122, 120, and

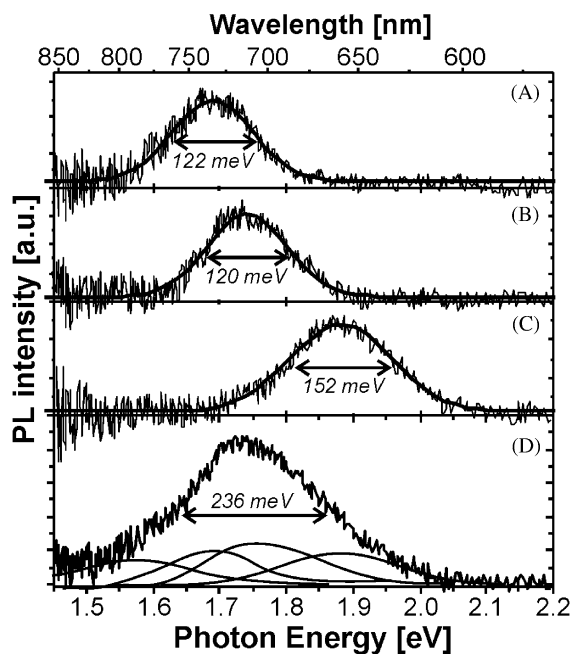


Fig. 3. PL spectra of three different single Si-NCs under 325 nm excitation (0.5 W/cm^2) at RT (panels A–C). The bold smooth lines are Gaussian fits (FWHM is 122, 120 and 152 meV for dots A, B and C, respectively). Panel D shows a sum of 9 spectra of different single NCs from one sample. Four of these individual spectra (smoothed out) are shown under the sum spectrum.

152 meV for spectra of dots A, B, and C, respectively. The bottom part of Fig. 3 shows a sum of 9 spectra of individual dots measured under identical conditions in one sample. As expected, this ensemble spectrum is significantly broader than individual spectra.

According to the experimental data of Wolkin et al. [1] and calculations of Reboredo et al. [13], a PL maximum at 1.7 eV corresponds to a NC diameter of about 3.6 nm. However, we are still unable to confirm the size of the Si-core of a luminescing single-NC by direct measurement.

Under increasing excitation intensity, the emission band is slightly broadened and a spectral structure appears but only for some NCs. Five spectra detected under excitation intensity increasing from 0.03 to 0.5 W/cm^2 are plotted in Fig. 4. The inset shows integrated PL intensity as a function of excitation intensity. The PL starts to saturate for excitation intensities above 0.3 W/cm^2 . The spectral structure has a form of a quasi-periodic modulation of the PL intensity with a period of about 80 meV.

Fluctuations of the PL signal from single Si-NCs were studied by repeated detection of PL

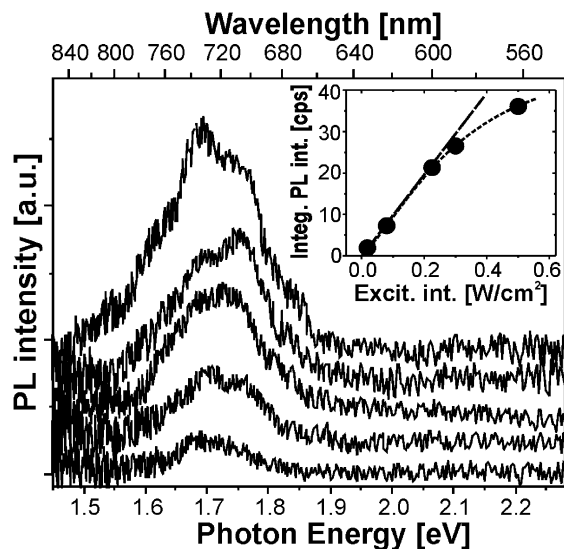


Fig. 4. Intensity dependence of the spectral shape for an efficiently emitting NC: Excitation intensity increases from 0.03 to 500 mW/cm^2 . Corresponding integral PL intensities are shown in the inset as a function of excitation intensity.

images with exposure time of 1 min. This is the shortest detection time necessary to obtain a reasonable signal-to-noise ratio. In Fig. 5, the integrated PL signal from four individual dots is plotted. Despite, the quite long detection time one can see relatively large fluctuations of the PL intensity for certain NCs (e.g. dots (b) and (e) in Fig. 5), whereas some NCs (e.g. dot (a) in Fig. 5) appear stable (i.e. variations within detection noise, background signal being ~ 30 counts/min). (The upper panel of Fig. 5 shows a PL image of a part of the sample with indicated positions of dots whose emission properties are reported in Figs. 5 and 6.) Let us note that PL fluctuations are stronger for NCs showing lower averaged emission intensity (e.g. dots (d) and (e) in Fig. 5) and that dot (e) is completely turned off towards the end of measurement. We can speculate that observed PL intensity fluctuations originate in PL intermittence (on–off switching) which is often observed in single NCs and molecules on the time scale of

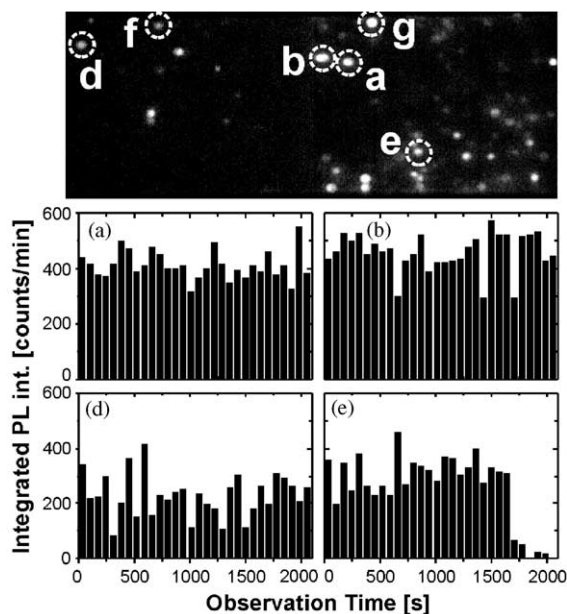


Fig. 5. Temporal stability of single Si-NC emission: Integrated PL intensity measured in 30 consecutive 1 min acquisitions is plotted against time. Dots (a), (b), (d), and (e) are presented in the four panels. The upper part of the figure is a PL image of a part of the sample with circles and labels corresponding to NCs presented in Figs. 3, 5 and 6.

seconds and millisecond (see, e.g. [14] for intermittence study in CdSe NCs).

Finally, we present polarization sensitive detection of single NC PL using a linear polarization filter (analyzer) inside a microscope (see schematic drawing in Fig. 6). This configuration allows checking the projection of an emitting dipole in the plane parallel to the sample surface. The results shown in Fig. 6 indicate that PL from a

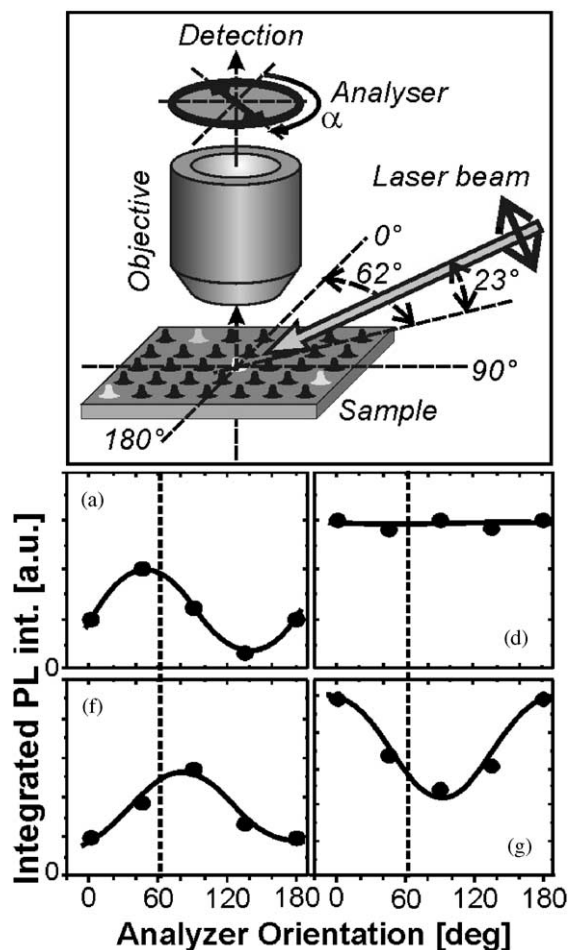


Fig. 6. Polarization selective detection of PL from single NCs: Integrated PL signal from dots (a), (d), (f), and (g) are plotted as a function of the analyzer orientation. Experimental data are fitted by a squared sinusoid. The dashed lines mark the angle corresponding to projection of the excited beam polarization. The top panel is a schematic drawing of the experimental configuration.

majority of individual NCs has a high degree of linear polarization. On the other hand, there is almost no polarization memory, i.e., the orientation of PL polarization is independent of the exciting beam polarization (projected at $\alpha = 62^\circ$ —indicated by dotted lines in Fig. 6).

The high degree of linear polarization indicates that the orientation of an emitting dipole is quite stable. This suggests that NCs showing polarized PL are elongated in different directions [15] whereas NCs with non-polarized PL has either a random orientation of the emitting dipole (spherical shape) or the dipole is oriented perpendicularly to the sample surface. The absence of a polarization memory could be explained by the high energy of excitation—far from the emission wavelength. Thus, the absorbing and emitting states are very different.

4. Discussion

4.1. Shape of the PL spectrum of a single Si-NC

The bandwidth of PL spectra (120–210 meV), we observe in single Si-NCs is very large. Other semiconductor NCs have also broad PL bands when studied at RT but still few times narrower than in our case (see for example [14], where the single CdSe NC has FWHM of PL band ~ 50 meV at RT, but few meV or less at 15 K).

There are mainly two reasons for the wide PL spectrum: dominating phonon-assisted transitions and spectral diffusion.

As we mentioned before Si-NCs conserve the indirect band gap. Therefore, one or more phonons have to take part in optical transitions in order to conserve momentum [7]. Recently, theoretical studies have shown that phonon-assisted transitions in Si-NC dominate over full range of sizes and even at low temperature [16]. Participation of several phonons in radiative recombination of electron–hole pairs could also explain the quasi-periodic structure we observed for some dots (see Fig. 4). The period of about 80 meV does not correspond to any phonon energy in bulk Si (for optical transition LO-phonon dominate—its energy in the Γ -point of bulk Si at

RT 64.4 meV) but it could be a surface phonon or local vibration energy. Further studies are under way.

We have to stress that the detection time for a PL spectrum from a single Si-NC is 30 min. Therefore, the inherent phonon-related structure of PL spectra can be smoothed out by spectral diffusion. Spectral diffusion is a shift of the emission line due to the variations of local field. It was observed in II–VI semiconductor QD that the line width is strongly dependent on the detection time as a consequence of important spectral diffusion even at low temperature [17].

It would be desirable to measure PL of single Si-NC also at low temperatures. However, such experiment will be very difficult as the PL photon rate is further reduced due to the increasing lifetime of Si-NC excited states.

4.2. PL quantum efficiency in single Si-NC

The well-defined experimental conditions allow us to estimate a PL quantum efficiency (QE) for the best emitting Si-NCs. We took two different approaches to calculate the QE.

The first method uses the PL signal well-below saturation. Let us take an excitation intensity of $P = 80$ mW/cm². The corresponding photon flux is 1.3×10^{17} photons/s/cm² (i.e. 10 times lower than the saturation limit as defined before). The fraction absorbed in one NC is determined by the absorption cross-section. This quantity was studied in detail by Kovalev and co-workers [7] in ensemble of Si-NCs. For excitation at 3.81 eV and detection at 1.65 eV they give $\sigma \sim 1 \times 10^{-14}$ cm². The signal count rate N is then equal to

$$N = D\eta\sigma P, \quad (1)$$

where η is the PL QE and D is the overall detection efficiency of photons emitted by a NC ($D = 0.026$ for our experimental setup). The most intense NCs produce count rates of about 12 counts/s under $P = 80$ mW/cm². This gives us a high QE of 35% (estimated accuracy is about $\pm 50\%$) for the best NCs. The majority of NCs seen in PL images in Figs. 2 and 5 have QE between 5% and 20%.

The second calculation uses saturated PL signal. This approach was adopted by Buratto's group to

calculate PL QE as high as 88% in individual grains of porous Si [10,11]. The saturated count rate is calculated using the equation:

$$N_{\text{sat}} = D\eta/\tau, \quad (2)$$

where τ is the excited state lifetime. For the NC used in the above-described calculation, we found N_{sat} about 40 cps for the highest excitation intensity we used. Using lifetime $\tau = 100 \mu\text{s}$ (taken from measurements on ensemble of Si-NCs [8]) Eq. (2) yields a QE of 15% which corresponds well with the value obtained from Eq. (1). (However, the excited state lifetime may be significantly different in the present structures.)

Finally, let us note that only a few percent of Si-NCs in our structures show detectable PL, cf. Fig. 2b. This is in agreement with the report by Mason et al. that only about 2.8% of porous Si particles are luminescing [9]. The reason could be non-radiative quenching by defects eventually escape of electron–hole pairs to the substrate. Indeed, the critical effect of defect passivation was clearly illustrated by the fact that the PL was totally quenched following the electron beam exposure during SEM imaging and could only be regained by a forming gas anneal. Therefore, better isolation of NCs from the substrate and different oxidation conditions and forming-gas anneals are clearly worth to study. Whether it is possible to increase the fraction of luminescing dots and their QE or if the statistical nature of the occurrence of defects in NCs puts an upper limit to these numbers, remains unanswered.

In conclusion, we have demonstrated that the imaging spectroscopy is applicable for single QD photoluminescence measurement even in the case of very low emission rate typical for Si-NCs.

We have prepared regular lattices of Si nanopillars that were oxidized effectively which result in oxide covered 0-D Si-NCs. Individual nanopillars were resolved in a far-field optical microscope. Their PL emission was imaged and PL spectra detected at RT. There is a good spatial coincidence of the reflection and PL signal from the nanopillar structure. The conjecture that we observe PL emission of single Si-NCs is further supported by the PL spectral shape and strong temporal fluctuation of PL signal from a NC. The spectra

have approximately Gaussian shape (sometimes with a quasi-periodic structure) and FWHM in the range of 120–210 meV (clearly narrower than ensemble spectra).

The quantum efficiency of PL was found about 35% in the best Si-NCs but only a few percent of the total number of NCs show a detectable PL signal. We have demonstrated significant PL fluctuations in time. PL emission was shown to have high degree of linear polarization in many NCs, which suggest elongated non-spherical shape of NCs.

The unique regular arrangement of Si-NCs allows for repeated retrieval and measurement of a specific individual NC. In future, such samples could be effectively used to study for example the effects of shape or surface modifications on the PL of Si-NCs.

Acknowledgements

The authors would like to acknowledge discussions on the experimental parts with S. Empedocles, A. Galeckas, and M. Vácha and express their gratitude for being able to use e-beam lithography at Chalmers and at the KTH nanolab. Partial funding was received from the KTH Faculty and the European SBLED project. JV acknowledges support from GAAV CR project B1112901.

References

- [1] M.V. Wolkin, J. Jorne, P.M. Fauchet, G. Allan, C. Delerue, *Phys. Rev. Lett.* 82 (1999) 197.
- [2] W.L. Wilson, P.F. Szajowski, L.E. Brus, *Science* 262 (1993) 1242.
- [3] A. Gustafsson, M-E. Pistol, L. Montelius, L. Samuelson, *J. Appl. Phys.* 84 (1998) 1715.
- [4] S.A. Empedocles, D.J. Norris, M.G. Bawendi, *Phys. Rev. Lett.* 77 (1996) 3873.
- [5] M-E. Pistol, P. Castrillo, D. Hessman, J.A. Prieto, L. Samuelson, *Phys. Rev. B* 59 (1999) 10725.
- [6] S.A. Empedocles, M.G. Bawendi, *Science* 278 (1997) 2114.
- [7] D. Kovalev, K. Heckler, G. Polisski, F. Koch, *Phys. Status Solidi B* 215 (1999) 871.
- [8] J. Linnros, N. Lalic, A. Galeckas, V. Grivickas, *J. Appl. Phys.* 86 (1999) 6128.
- [9] M.D. Mason, G.M. Credo, K.D. Weston, S.K. Buratto, *Phys. Rev. Lett.* 80 (1998) 5405.

- [10] G.M. Credo, M.D. Mason, S.K. Buratto, *Appl. Phys. Lett.* 74 (1999) 1978.
- [11] M.D. Mason, D.J. Sirbuly, P.J. Carson, S.K. Burrato, *J. Chem. Phys.* 114 (2001) 8119.
- [12] H.I. Liu, D.K. Biegelsen, F.A. Ponce, N.M. Johnson, R.F.W. Pease, *Appl. Phys. Lett.* 64 (1994) 1383.
- [13] F.A. Reboledo, A. Franceschetti, A. Zunger, *Phys. Rev. B* 61 (2000) 13073.
- [14] U. Banin, M. Bruchez, A.P. Alivisatos, T. Ha, S. Weiss, D.S. Chemla, *J. Chem. Phys.* 110 (1999) 1195.
- [15] G. Allan, C. Delerue, Y.M. Niquet, *Phys. Rev. B* 63 (2001) 205301.
- [16] C. Delerue, G. Allan, M. Lannoo, *Phys. Rev. B* 64 (2001) 193402.
- [17] S.A. Empedocles, D.J. Norris, M.G. Bawendi, *Phys. Rev. Lett.* 77 (1996) 3873.